Cell Reports
Report

Nutrient Deprivation Elicits a Transcriptional and Translational Inflammatory Response Coupled to Decreased Protein Synthesis

Paulo A. Gameiro[1,2] and Kevin Struhl[1,3,*]
[1]Department of Biological Chemistry and Molecular Pharmacology, Harvard Medical School, Boston, MA 02115, USA
[2]Present address: Department of Molecular Neuroscience, UCL Institute of Neurology, 10-12 Russell Square House, London WC1B 5EH, UK
[3]Lead Contact
*Correspondence: kevin@hms.harvard.edu
https://doi.org/10.1016/j.celrep.2018.07.021

SUMMARY

Nutrient deprivation inhibits mRNA translation through mTOR and eIF2α signaling, but it is unclear how the translational program is controlled to reflect the degree of a metabolic stress. In a model of breast cellular transformation, various forms of nutrient deprivation differentially affect the rate of protein synthesis and its recovery over time. Genome-wide translational profiling of glutamine-deprived cells reveals a rapid upregulation of mRNAs containing uORFs and downregulation of ribosomal protein mRNAs, which are followed by selective translation of cytokine and inflammatory mRNAs. Transcription and translation of inflammatory and cytokine genes are stimulated in response to diverse metabolic stresses and depend on eIF2α phosphorylation, with the extent of stimulation correlating with the decrease in global protein synthesis. In accord with the inflammatory stimulus, glutamine deprivation stimulates the migration of transformed cells. Thus, pro-inflammatory gene expression is coupled to metabolic stress, and this can affect cancer cell behavior upon nutrient limitation.

INTRODUCTION

An adequate nutrient supply is essential for optimal mRNA translation, and eukaryotic cells have evolved nutrient-sensing pathways that coordinate protein synthesis with nutritional status. Nutrient deprivation inhibits global protein synthesis through modulation of the mechanistic target of rapamycin (mTOR) (Wullschleger et al., 2006) and integrated stress response (ISR) pathways (Holcik and Sonenberg, 2005).

The mTOR signaling pathway integrates nutritional and energy signals to regulate global translational rates via phosphorylation of 4E-BP1 and S6K1, both of which are important for cap-dependent translation (Wullschleger et al., 2006). In addition, mTOR preferentially regulates mRNAs containing TOP motifs in their 5′ UTR, which often encode ribosomal proteins that are translationally repressed in an mTOR-dependent manner (Tang et al., 2001; Thoreen et al., 2012).

In the ISR pathway, diverse stresses lead to the phosphorylation of the translation initiation factor eIF2α by four kinases, each of which is activated by specific stresses (Holcik and Sonenberg, 2005). Phosphorylation of eIF2α generally inhibits translation, but it enhances the translation of specific mRNAs, such as that encoding the transcription factor ATF4 or its yeast counterpart Gcn4 (Harding et al., 2000; Holcik and Sonenberg, 2005). Translational control of ATF4 is mediated by short upstream open reading frames (uORFs) that block translation of the downstream canonical ORF during normal growth but permit the scanning ribosome to initiate translation at the canonical ORF under starved conditions (Vattem and Wek, 2004). Selective translation of ATF4 is responsible for the transcriptional activation of adaptation genes under amino acid deprivation (Harding et al., 2003).

As dividing cells rely differently on glucose (Bauer et al., 2004; Warburg et al., 1927), glutamine (DeBerardinis et al., 2007; Newsholme et al., 1985), glycine (Jain et al., 2012), serine (Maddocks et al., 2013), and leucine (Sheen et al., 2011) to support specific metabolic functions, deprivation of some nutrients may impose more severe constraints on mRNA translation than others. In addition, oncogenes can drive translation of specific mRNAs involved in cell growth, metabolism, invasion, and metastasis (Truitt and Ruggero, 2016). However, there is limited knowledge about how different metabolic stresses control mRNA translation and how the translational program is linked to the degree of metabolic stress. Here, we show that a variety of nutrient stresses lead to an inflammatory response, at both the transcriptional and translational levels, that is linked to inhibition of global protein synthesis.

RESULTS

Nutrient Limitation Differentially Affects Nascent Protein Synthesis

We analyzed the response to nutrient limitation in a model of cellular transformation that involves an immortalized breast epithelial cell line (MCF10A) containing an endoplasmic reticulum (ER)-Src fusion gene consisting of the v-Src oncogene and the ligand-binding domain of the estrogen receptor (Hirsch et al., 2010; Iliopoulos et al., 2009). Treatment of these cells with tamoxifen activates Src, which generates a rapid

inflammatory stimulus causing an epigenetic switch from a non-transformed state to a stable transformed state (Iliopoulos et al., 2009). Using a fluorescent methionine analog, we quantified *de novo* protein synthesis in cells subjected to short-term (30 min) deprivation of glucose or amino acids with different bioenergetic functions. With the exception of glycine and serine deprivation, protein synthesis is inhibited to various extents depending on the limiting nutrient (Figures 1A and 1B), with deprivation of branched-chain amino acids (BCAAs) having the strongest effect. Protein synthesis is reduced in transformed cells, though the relative effects for the various nutrient stresses are similar in both cell types.

To analyze how cells recover from nutrient deprivation, we measured protein synthesis after 4 and 6 hr of nutrient deprivation (Figure 1C). Protein synthesis returns to normal or near-normal levels upon deprivation of cysteine + cysteine or of glucose, presumably due to metabolic adaptations. In contrast, cells deprived of BCAAs and glutamine recover poorly, presumably because they cannot synthesize these amino acids to sufficient levels. In all these cases, non-transformed and transformed cells behave similarly, though transformed cells seem to recover less well under glutamine deprivation (Figure 1C). The importance of glutamine in cancer cell metabolism (Altman et al., 2016) prompted us to investigate the translational program of transformed and non-transformed cells subjected to glutamine deprivation.

The Immediate Translational Response to Glutamine Deprivation: Downregulation of mRNAs Involved in Translation and Upregulation of mRNAs Containing uORFs

We performed ribosome profiling (Ingolia et al., 2012), sequencing of ribosome-protected RNA, on transformed and non-transformed cells cultured with either complete or glutamine-depleted medium for 30 min. Using RibORF (Ji et al., 2015), we identified ~5 million unique exon-mapped, ribosome footprints corresponding to ~5,700 translated ORFs (Table S1). For each mRNA, we $\log_2$ divided the reads per kilobase of transcript per million mapped reads (RPKM) measured by ribosome profiling over the RPKM measured by RNA sequencing (RNA-seq) to obtain translation efficiencies (TEs), and then determined differential TE induced by glutamine deprivation. We also analyzed the ribosome occupancy (RO) as determined by the RPKM of ribosome-protected mRNA fragments. Approximately 140 mRNA transcripts have 1.5-fold or lower TE values, and these translationally inhibited mRNAs are enriched for ribosomal and translation proteins (Figures 2A and S1A), and most of them contain TOP motifs in their 5′ UTRs (Figure S1B). This regulatory response resembles that observed upon inhibiting TOR activity (Thoreen et al., 2012).

Conversely, only 13 (non-transformed cells) or 22 (transformed cells) mRNAs are translationally stimulated after 30 min of glutamine deprivation (Figure 2A), the most dramatic of which encodes ATF4. Like ATF4, some upregulated transcripts are linked to translational control and have translated uORFs. PPP1R15B (2 uORFs) is a phosphatase that dephosphorylates eIF2α, AZIN1 (6 uORFs) is an antizyme inhibitor that stimulates polyamine levels necessary for mRNA translation, and SAT1 (2 uORFs) inhibits translation through polyamine depletion. ATF4 and SAT1 are the only uORF-containing mRNAs upregulated in both transformed and non-transformed cells.

Selective Translation of Cytokine and Inflammatory mRNAs upon Glutamine Deprivation

To investigate the gene expression program during the recovery from glutamine deprivation, we performed ribosome and mRNA profiling of cells cultured for 4 hr with and without glutamine (Table S1). In contrast to the 30-min response (Figure 2A), the fold changes in mRNA and ribosome occupancy are strongly correlated (Figure 2B), indicating a strong transcriptional contribution to the response following 4 hr of glutamine deprivation. In addition, the cells are still metabolically stressed, as evidenced by decreased translational efficiency of ribosomal proteins and increased translational efficiency of ATF4 (Figure 2B).

Interestingly, 34 and 56 mRNAs are translated more efficiently in transformed and non-transformed cells (Figure 2B), respectively, and these are enriched for genes involved in cytokine activity, inflammation, and angiogenesis (Figures 2B and 2C; Table S2). Some cytokines and inflammatory mRNAs are induced transcriptionally but do not show increased TE (Figure 2B; Table S2). As TE values tend to be correlated with cytosolic mRNA levels (Larsson et al., 2010), we also performed an analysis of the partial variance (APV) of ribosome occupancy and mRNA levels to identify differential translation with higher sensitivity (Larsson et al., 2010). The APV shows increased translation of cytokine mRNAs mainly in transformed cells (Figure 2C) and increased ribosome occupancy (combined transcription and translation) of inflammatory mRNAs in both cell types (Figure S1C; Table S2). As expected from the induction of the ISR pathway, the mRNAs with increased ribosome occupancy are also involved in the ER stress response, which includes the transcription factors DDIT3 and XBP1, the canonical targets CHAC1 and PPP1R15A, and aminoacyl-tRNA synthetases (Figure 2B and S1C). Non-transformed cells also exhibit increased expression of cytokine and angiogenic mRNAs, but this response is less pronounced and, primarily, transcriptionally mediated (Figures 2B, S1C, and S1D; Table S2). Thus, glutamine deprivation stimulates inflammatory mRNAs, and this response is both transcriptionally and translationally enhanced in transformed cells.

Although MCF10A cells express glutamine synthetase (GLUL) and can proliferate without glutamine supplementation in the medium, GLUL is not regulated by glutamine deprivation (Figure 2D). In contrast, genes involved in glutamine catabolism, such as glutaminase (GLS) and glutamate-oxaloacetic transaminase 1 (GOT1), are induced (Figure 2D). In general, genes encoding enzymes in the tricarboxylic acid (TCA) cycle are mostly unaffected by glutamine deprivation.

Cytokine and Inflammatory Gene Expression Is Coupled to Translational Inhibition upon Nutrient Deprivation

We performed similar experiments in cells subjected to 4 hr of deprivation of glucose, cysteine/cystine, and BCAA. As observed upon glutamine deprivation, cytokine and inflammatory mRNAs are enhanced at both the transcriptional and TE levels upon deprivation of BCAA (Figures 3A and S2A; Table S2). Cells deprived of glucose or cysteine/cystine-deprived cells

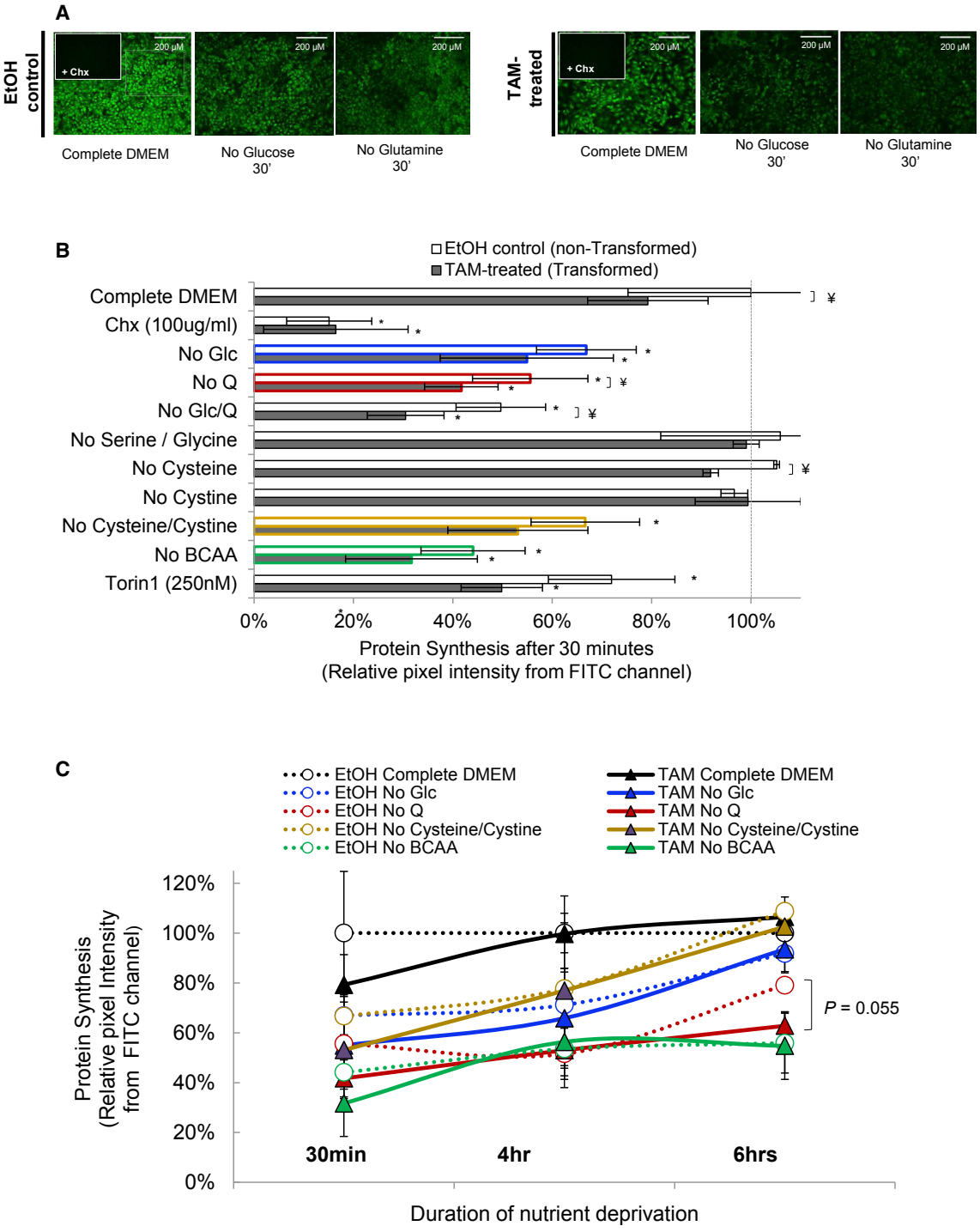

Figure 1. Quantification of Protein Synthesis in Response to Metabolic Stresses

(A) Nascent proteins containing the "clickable" methionine analog (AHA) visualized by fluorescence microscopy.

(B) Quantification of nascent protein synthesis in tamoxifen (TAM)-treated and EtOH control cells under different metabolic conditions. CHX, cycloheximide.

(C) Recovery of nascent protein synthesis over time.

Error bars represent SD of three or more biological replicates, except for the 6-hr samples, and no cysteine or cystine at 30 min (two biological replicates). *$p < 0.05$, comparing nutrient-deprived to complete medium; ¥$p < 0.05$, comparing TAM-treated to EtOH control cells, as determined by t test. FITC, fluorescein isothiocyanate.

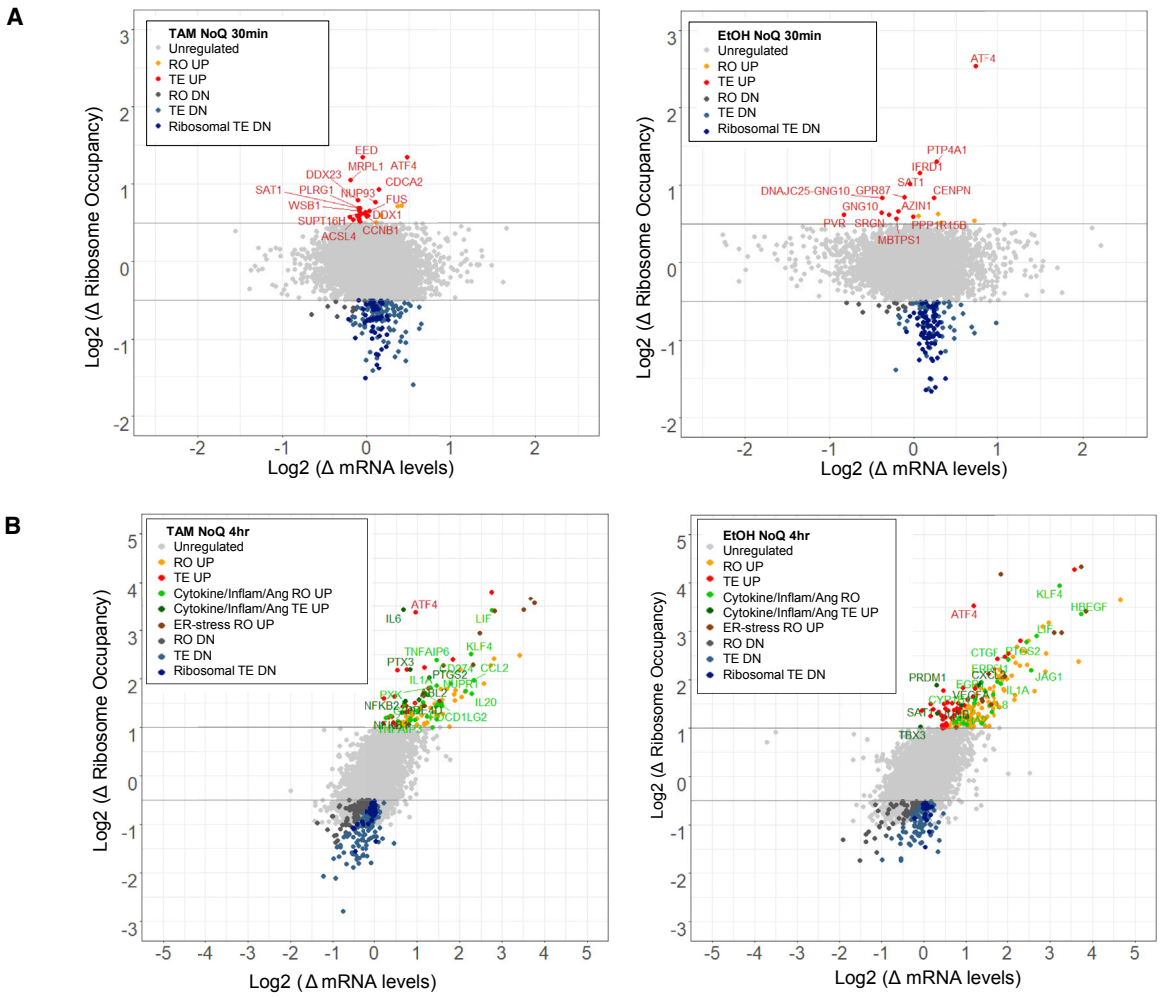

C

TAM-treated – NoQ 4hrs				
Analysis by Log2 TE fold change				
term ID	description	log_{10} p-value	dispensability	N genes
GO:0001819	positive regulation of cytokine production	-2.85	0.00	7
GO:0034613	cellular protein localization	-2.30	0.00	11
GO:0060429	epithelium development	-2.37	0.00	10
GO:0071496	cellular response to external stimulus	-3.09	0.00	7
GO:0072593	reactive oxygen species metabolic process	-2.85	0.00	6
GO:2001057	reactive nitrogen species metabolic process	-2.75	0.01	4
Analysis by Anota2seq – "Translation Mode"				
term ID	description	log_{10} p-value	dispensability	N genes
GO:0001819	positive regulation of cytokine production	-3.21	0.00	6
GO:0006094	gluconeogenesis	-2.29	0.06	3
GO:0006984	ER-nucleus signaling pathway	-2.98	0.16	3
GO:1901214	regulation of neuron death	-2.17	0.18	4
GO:0030155	regulation of cell adhesion	-2.68	0.19	6
GO:0051270	regulation of cellular component movement	-2.37	0.20	6

D

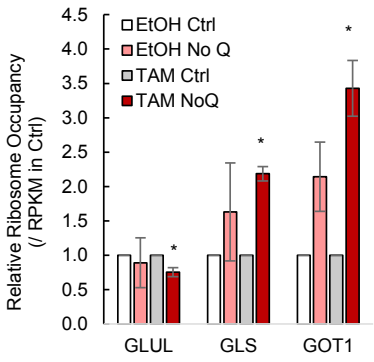

Figure 2. Regulation of mRNAs upon Glutamine Deprivation

(A) Changes in mRNA and ribosome occupancy levels upon 30-min deprivation of glutamine relative to complete medium in transformed (left) and non-transformed (right) cells.

(B) Similar analysis in cells grown for 4 hr in glutamine-deprived versus complete medium.

(legend continued on next page)

behave similarly, although to a lesser extent (Figures S2B and S2C). In contrast to the 30-min dataset, the 22 inflammatory mRNAs with increased TE in all stresses (Figure S2D) do not contain many uORFs (Figure S2E; Table S2). As also determined by the APV model, the overall inflammatory response by nutrient depletion is induced both at the transcriptional level (Figure 3B) and translational level (Figure 3C), and it is more pronounced in the transformed state. Intriguingly, stresses causing the strongest inhibition of protein synthesis after 30 min and weakest recovery at 4 and 6 hr (Figure 1, depletion of glutamine or BCAA) also cause the most pronounced increase in cytokine and inflammatory expression (Figures 3D and S2F). In addition, the number of TE-downregulated mRNAs is higher in more "severe" stresses (Figures 2B, 3A, S2B, and S2C).

To examine more rigorously whether increased cytokine expression is linked to translational stress, we performed hierarchical clustering of all conditions based on ribosome occupancy (Figure 3E). Aggregation of all mRNAs into five k-means clusters shows that cytokine and inflammatory mRNAs are highly co-regulated among the metabolic conditions with the highest upregulation in BCAA and glutamine-deprived transformed cells and the lowest expression in non-transformed cells grown with complete, cysteine/cystine- or glucose-free DMEM (Figure 3F; Table S2, cluster 2). Conversely, the cluster with the strongest downregulation in BCAA and glutamine-deprived transformed cells is strongly enriched for ribosomal proteins (Figure 3F; Table S2, cluster 5). Cluster 1 consists of immune-related mRNAs and is, overall, upregulated in transformed cells (Iliopoulos et al., 2009). In addition, recovery of protein synthesis 6 hr after the stress is inversely correlated with the geometric mean in ribosome occupancy of 12 cytokines (Figure 3G; Table S2), but not with aminoacyl-tRNA synthetases, whose transcription is induced by amino-acid deprivation (Figure S3A), or ATF4, the canonical example of selective mRNA translation (Figure S3B). Likewise, the ribosome occupancy of all downregulated mRNAs (Figure 3H) and 176 ribosomal factor mRNAs in Gene Ontology (GO): 0003735 (Figure S3C) is lower in the more severe stresses, though the pattern is less evident for the latter, as ribosomal factor mRNAs are proportionally more represented in the glucose stress (Figure S3D).

Enhanced Cytokine Expression Requires Translational Inhibition by eIF2α Phosphorylation

To examine whether inhibition of protein synthesis, per se, leads to an inflammatory response, we performed ribosome profiling of transformed cells treated with torin1, an inhibitor of mTOR. As expected (Thoreen et al., 2012), and in accord with what occurs upon nutrient depletion, torin1-treated cells show decreased levels of protein synthesis (Figure 1B), with translation of ribosomal proteins being particularly affected (Figure 4A). Nutrient deprivation mitigates the phosphorylation of 4EBP1 and S6K1 at 30 min and 4 hr to different extents (Figures 4B and S4A). However, in contrast to conditions of nutrient depletion, torin1 markedly inhibits the phosphorylation of mTOR targets at 30 min and 4 hr (Figures 4B and S4A) but does not lead to increased translation of inflammatory genes (Figure 4A). Indeed, the TE of some cytokine mRNAs actually decreases upon torin1 treatment, and the level of transcriptional induction is considerably below what occurs upon nutrient stresses.

In accord with these observations, eIF2α phosphorylation increases upon all forms of nutrient deprivation tested here, but it is not affected by torin1 treatment (Figure 4B). In addition, non-stressed transformed cells exhibit higher levels of eIF2α phosphorylation and lower levels of protein synthesis than non-transformed cells (Figure 4B). To test whether the inflammatory response is linked to eIF2α phosphorylation, we measured cytokine levels in nutrient-deprived cells treated with ISRIB, a potent inhibitor of the integrated stress response pathway (Sidrauski et al., 2013). Cytokine protein levels are induced after glutamine depletion and in response to the other amino-acid stresses (Figure S4B). Treatment with the ISRIB inhibitor decreases the induced expression of IL8, IL6, and CCL20 in transformed cells, and of IL8 in non-transformed cells, after 4 hr of glutamine deprivation (Figure 4C). In accord with the literature, ISRIB does not affect the levels of phosphorylated eIF2α (Sidrauski et al., 2013). Thus, translational repression by eIF2α phosphorylation is necessary for the enhanced cytokine expression under metabolic stress.

Short-Term Nutrient Deprivation Increases Cell Migration

As secreted chemokines can induce the directed migration of leukocytes and neighbor cells, we examined whether glutamine deprivation affects cell migration. Migration of transformed cells through a basement membrane is enhanced toward conditioned medium (CM) from glutamine-deprived cells relative to fresh glutamine-depleted medium, whereas complete CM inhibits cell migration when compared to fresh complete medium (Figure 4D). Migration of non-transformed cells is not affected through the basement membrane (Figure 4D), but their motility is enhanced in a wound healing assay in CM from glutamine- or BCAA-deprived cells (Figure S4C). Transformed cells do not exhibit increased motility in the wound-healing assay (Figure S4C). Thus, short-term glutamine deprivation can drive cancer cell behavior independently of proliferation.

DISCUSSION

As defined by the resulting gene expression patterns, depletion of nutrients with different metabolic functions cause similar, but not identical, inflammatory responses in transformed and non-transformed cells at the transcriptional and translational levels. It is likely that the transcriptional response involves the transcription factor NF-κB (nuclear factor κB), as glutamine deprivation leads to increased NF-κB activity (Hou et al., 2012; Kim et al. 2014). Conversely, glutamine supplementation

(C) GO analysis of translationally regulated mRNAs as determined by $\log_2$ TE (top) and APV by anota2seq (bottom).
(D) Relative RO of glutamine-catabolizing enzymes.
Error bars represent SD of two biological replicates. *$p < 0.05$, comparing glutamine-deprived to complete medium, as determined by t test.
See also Figure S1.

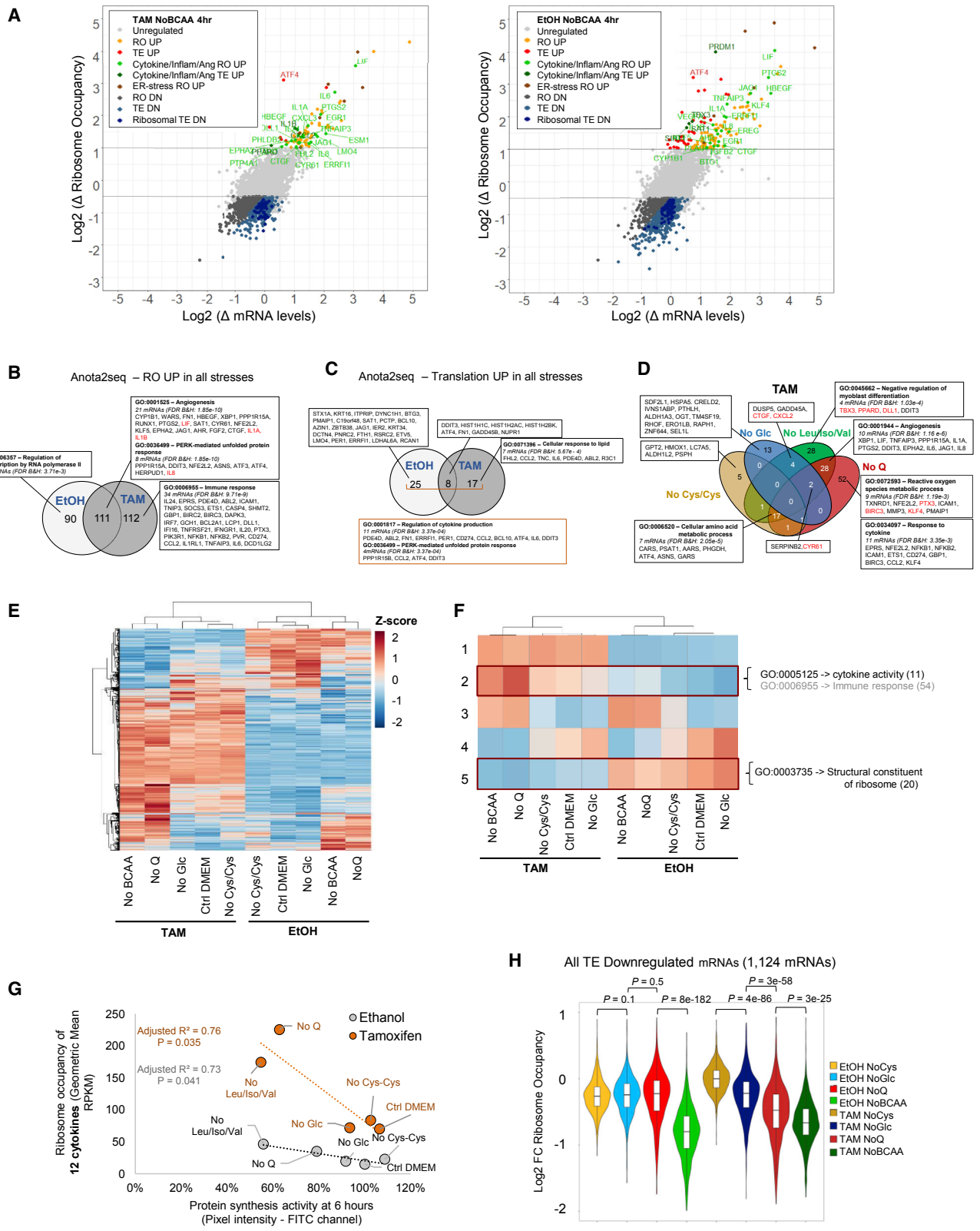

(legend on next page)

prevents NF-κB activity and cytokine expression (Chen et al., 2008; Singleton et al., 2005). Glutamine deprivation also triggers co-localization of autophagosomes, lysosomes, and the Golgi apparatus into a subcellular structure whose integrity is essential for IL-8 secretion, a process regulated by mTOR and JNK kinases (Shanware et al., 2014).

Translational stimulation of cytokine and inflammatory mRNAs upon nutrient or other stresses has not been described previously. However, based on published ribosome profiling data, we noticed that cells treated with thapsigargin (Reid et al., 2014), a drug that induces ER stress, show increased translation of inflammatory mRNAs. Our observation that nutrient (and, more generally, ER) stress affects inflammatory genes at both the transcriptional and translational levels underscores the biological importance of this response.

The relationship between the inflammatory response and metabolic stress is relevant to transformed cells. First, as NF-κB and STAT3 are critical for inflammation and tumor development (Grivennikov et al., 2010), increased inflammation in transformed cells is likely to have a greater impact in nutrient-deprived tumors than in normal tissues. As the concentrations of glucose and glutamine are lower in tumors than in normal tissues (Cairns et al., 2011; Warburg et al., 1927), pro-inflammatory translation may be enhanced in a tumor microenvironment. Second, increased expression of cytokines in a nutrient-limited environment would be an autocrine mechanism for tumor cells to invade and metastasize. As glutamine depletion, per se, negatively modulates cell migration, cytokine production under this condition might permit cancer cells to migrate toward a region with higher glutamine concentration. In addition, breast cancer cells selected to grow in the absence of glutamine become more metastatic and tumorigenic and overexpress cyclooxygenase-2 (COX-2 or PTGS2) (Singh et al., 2012), one of the more efficiently translated mRNAs in glutamine-deprived cells in our experiments.

The inverse relationship between the inflammatory response and general protein synthesis suggests a mechanistic connection between these two processes. Inhibition of mTOR activity induces eIF2α phosphorylation in a context-dependent manner (Cherkasova and Hinnebusch, 2003; Gandin et al., 2016; Thoreen et al., 2009; Wengrod et al., 2015). Inhibition of mTOR does not explain our findings, because torin1 decreases protein synthesis to an extent comparable to that of many conditions of nutrient depletion but does not lead to a similar inflammatory response. In fact, torin1-treated cells exhibit a lower translation of various cytokine and inflammatory mRNAs, so basal mTOR activity is probably required for the inflammatory response. In contrast, ISRIB reverses the effects of eIF2α phosphorylation (Sidrauski et al., 2013) and diminishes enhanced cytokine expression in glutamine-deprived cells, suggesting that inhibition of translation initiation by eIF2α phosphorylation triggers the inflammatory response. eIF2α phosphorylation leads to activation of NF-κB due to decreased levels of the IκB inhibitor arising from the combination of its short half-life and the reduced translation (Deng et al., 2004; Jiang et al., 2003). This mechanism may explain why the transcriptional induction of cytokines does not occur rapidly upon nutrient deprivation but, rather, takes several hours.

The inflammatory response arising upon nutrient depletion also occurs at the translation level. Though unknown, the mechanistic basis of this translational control likely involves eIF2α phosphorylation and may act in a uORF-independent manner, as 15 of the 22 TE upregulated inflammatory mRNAs do not contain uORFs. Cytokine mRNAs can be stabilized by the mitogen-activated protein (MAP) kinase/p38 pathway via au-rich element (ARE)-binding proteins that interact with sequences within the 3′ UTR (Hoffmann et al., 2002), so ARE- or other RNA-binding proteins might interact with translation factors and/or ribosomes to affect the translation of cytokine mRNAs. Whatever the precise mechanisms involved, the opposing effects of eIF2α phosphorylation on general translation and inflammatory response provides a mechanism to coordinate these processes in response to a wide range of nutritional states.

EXPERIMENTAL PROCEDURES

Cell Culture

MCF10A-ER-Src cells were grown at 37°C with 5% CO_2 in phenol red-free DMEM-F12 medium containing 5% charcoal-stripped horse serum, penicillin-streptomycin (1×), epidermal growth factor (EGF) (200 ng/mL), hydrocortisone (0.5 μg/mL, final), cholera toxin (100 ng/mL), and insulin (10 μg/mL), as described previously (Iliopoulos et al., 2009). Cells were transformed by treatment with 1 μM 4-hydroxy-tamoxifen for 24 hr, and ethanol was used as vehicle control in non-transformed cells. For metabolic experiments, cells were grown in the same medium but lacking nutrients as indicated.

Measurement of Nascent Protein Synthesis

Protein synthesis was assessed by treating cells with the "clickable" methionine analog L-azidohomoalanine (AHA) for 30 min, 4 hr, or 6 hr and detecting nascent proteins by fluorescence microscopy using the 488-nm laser channel according to the manufacturer's instructions (Thermo Fisher Scientific, catalog no. C10289). Details are given in the Supplemental Experimental Procedures.

Ribosome Profiling and RNA-Seq

Details pertaining high-throughput sequencing data acquisition and analyses are given in the Supplemental Experimental Procedures. Ribosome profiling and RNA-seq were performed as described previously (Ingolia et al., 2012).

Figure 3. Regulation of mRNAs upon 4 hr of Metabolic Stress Conditions

(A) Changes in mRNA and ribosome occupancy levels upon 4-hr deprivation of BCAAs relative to complete medium in transformed (left) and non-transformed (right) cells. Ang, angiogenesis; DN, down-regulated; RO, ribosome occupancy; UP, up-regulated.

(B and C) Venn diagram showing the anota2seq analysis of mRNAs with increased (B) transcriptional and (C) translational activity in all metabolic stresses in transformed versus non-transformed cells.

(D) Venn diagram showing the mRNAs with increased ribosome occupancy in each metabolic stress condition in transformed cells; cytokines are highlighted in red in non-inflammatory GO terms.

(E and F) Shown here: (E) hierarchical and (F) k-means clustering of ribosome occupancy across metabolic conditions.

(G) Correlation between protein synthesis and ribosome occupancy of regulated cytokines among nutrient-deprived conditions.

(H) Ribosome occupancy of all TE-downregulated mRNAs in each metabolic condition; p values are derived from the Wilcoxon test.

See also Figures S2 and S3.

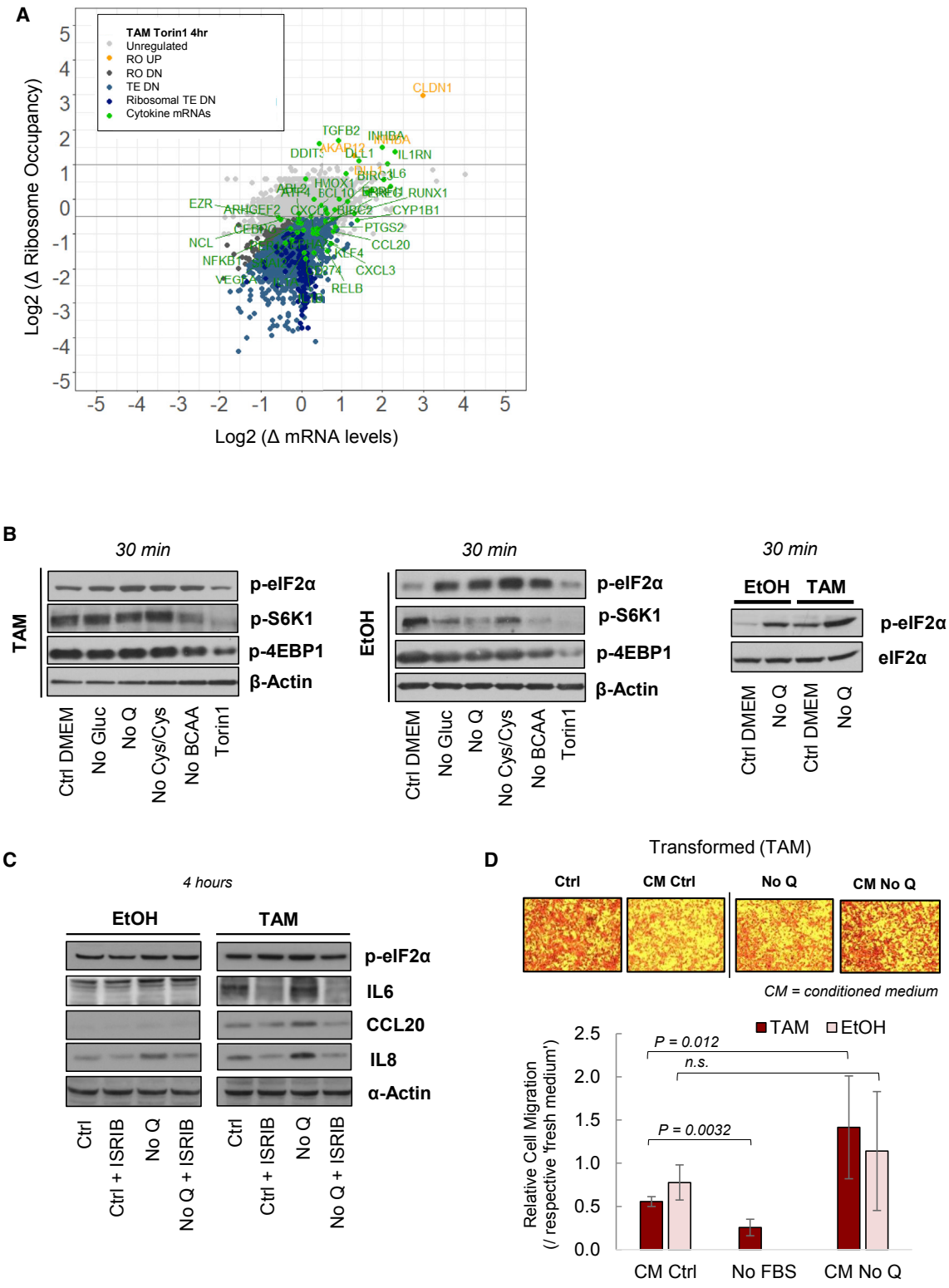

Figure 4. Cytokine Expression under Inhibition of mTOR and eIF2α Signaling and Migration of Glutamine-Deprived MCF10A-ER-Src Cells

(A) Changes in mRNA and ribosome occupancy levels in transformed cells subjected to 4-hr treatment with torin1 (500 nM) relative to complete medium.

(B) Immunoblot analysis of mTOR-phosphorylated proteins and eIF2α phosphorylation after 30 min of nutrient deprivation or Torin1 treatment (500 nM).

(legend continued on next page)

For determination of gene expression levels of protein-coding genes, we removed refSeq-defined coding regions overlapping with uORFs defined in Ji et al. (2015), 15 amino acids downstream of the start codons and 5 amino acids upstream of the stop codons. The gene expression levels were calculated as RPKMs in the remaining coding regions, and we considered only mRNAs expressed at RPKM > 10 in at least one of the metabolic conditions (Table S1). Differential translation was assessed by (1) TE, and (2) partial variance of RO and RNA levels (Larsson et al., 2010).

Statistical Analyses

Statistical analyses and visualizations were performed in R or Excel. The hierarchical and k-means clustering was performed using the pheatmap package with rlog-transformed ribosome occupancy. The association between protein synthesis and ribosome occupancy of cytokine mRNAs was tested using the Pearson correlation coefficient. Other statistical significance was assessed using either the Wilcoxon rank-sum test or t test, as indicated.

DATA AND SOFTWARE AVAILABILITY

The accession number for the sequencing data reported in this paper is GEO: GSE114794.

SUPPLEMENTAL INFORMATION

Supplemental Information includes Supplemental Experimental Procedures, four figures, and two tables and can be found with this article online at https://doi.org/10.1016/j.celrep.2018.07.021.

ACKNOWLEDGMENTS

We would like to thank Ji Zhe for help and expert advice with the RibORF pipeline and gene expression profile. This work was supported by grant CA 107486 to K.S. from the NIH.

AUTHOR CONTRIBUTIONS

Conceptualization and Resources, P.A.G. and K.S.; Methodology, Investigation, Validation, Formal Analysis, Data Curation, and Visualization, P.A.G.; Writing – Original Draft, P.A.G.; Writing – Review & Editing, P.A.G. and K.S.; Supervision, Project Administration, and Funding Acquisition, K.S.

DECLARATION OF INTERESTS

The authors declare no competing interests.

Received: November 22, 2017
Revised: May 22, 2018
Accepted: July 4, 2018
Published: August 7, 2018

REFERENCES

Altman, B.J., Stine, Z.E., and Dang, C.V. (2016). From Krebs to clinic: glutamine metabolism to cancer therapy. Nat. Rev. Cancer *16*, 773.

Bauer, D.E., Harris, M.H., Plas, D.R., Lum, J.J., Hammerman, P.S., Rathmell, J.C., Riley, J.L., and Thompson, C.B. (2004). Cytokine stimulation of aerobic glycolysis in hematopoietic cells exceeds proliferative demand. FASEB J. *18*, 1303–1305.

Cairns, R.A., Harris, I.S., and Mak, T.W. (2011). Regulation of cancer cell metabolism. Nat. Rev. Cancer *11*, 85–95.

Chen, G., Shi, J., Qi, M., Yin, H., and Hang, C. (2008). Glutamine decreases intestinal nuclear factor kappa B activity and pro-inflammatory cytokine expression after traumatic brain injury in rats. Inflamm. Res. *57*, 57–64.

Cherkasova, V.A., and Hinnebusch, A.G. (2003). Translational control by TOR and TAP42 through dephosphorylation of eIF2α kinase GCN2. Genes Dev. *17*, 859–872.

DeBerardinis, R.J., Mancuso, A., Daikhin, E., Nissim, I., Yudkoff, M., Wehrli, S., and Thompson, C.B. (2007). Beyond aerobic glycolysis: transformed cells can engage in glutamine metabolism that exceeds the requirement for protein and nucleotide synthesis. Proc. Natl. Acad. Sci. USA *104*, 19345–19350.

Deng, J., Lu, P.D., Zhang, Y., Scheuner, D., Kaufman, R.J., Sonenberg, N., Harding, H.P., and Ron, D. (2004). Translational repression mediates activation of nuclear factor kappa B by phosphorylated translation initiation factor 2. Mol. Cell. Biol. *24*, 10161–10168.

Gandin, V., Masvidal, L., Cargnello, M., Gyenis, L., McLaughlan, S., Cai, Y., Tenkerian, C., Morita, M., Balanathan, P., Jean-Jean, O., et al. (2016). mTORC1 and CK2 coordinate ternary and eIF4F complex assembly. Nat. Commun. *7*, 11127.

Grivennikov, S.I., Greten, F.R., and Karin, M. (2010). Immunity, inflammation, and cancer. Cell *140*, 883–899.

Harding, H.P., Novoa, I., Zhang, Y., Zeng, H., Wek, R., Schapira, M., and Ron, D. (2000). Regulated translation initiation controls stress-induced gene expression in mammalian cells. Mol. Cell *6*, 1099–1108.

Harding, H.P., Zhang, Y., Zeng, H., Novoa, I., Lu, P.D., Calfon, M., Sadri, N., Yun, C., Popko, B., Paules, R., et al. (2003). An integrated stress response regulates amino acid metabolism and resistance to oxidative stress. Mol. Cell *11*, 619–633.

Hirsch, H.A., Iliopoulos, D., Joshi, A., Zhang, Y., Jaeger, S.A., Bulyk, M., Tsichlis, P.N., Liu, X.S., and Struhl, K. (2010). A transcriptional signature and common gene networks link cancer with lipid metabolism and diverse human diseases. Cancer Cell *17*, 348–361.

Hoffmann, E., Dittrich-Breiholz, O., Holtmann, H., and Kracht, M. (2002). Multiple control of interleukin-8 gene expression. J. Leukoc. Biol. *72*, 847–855.

Holcik, M., and Sonenberg, N. (2005). Translational control in stress and apoptosis. Nat. Rev. Mol. Cell Biol. *6*, 318–327.

Hou, Y.-C., Chiu, W.-C., Yeh, C.-L., and Yeh, S.-L. (2012). Glutamine modulates lipopolysaccharide-induced activation of NF-κB via the Akt/mTOR pathway in lung epithelial cells. Am. J. Physiol. Lung Cell. Mol. Physiol. *302*, L174–L183.

Iliopoulos, D., Hirsch, H.A., and Struhl, K. (2009). An epigenetic switch involving NF-kappaB, Lin28, Let-7 microRNA, and IL6 links inflammation to cell transformation. Cell *139*, 693–706.

Ingolia, N.T., Brar, G.A., Rouskin, S., McGeachy, A.M., and Weissman, J.S. (2012). The ribosome profiling strategy for monitoring translation in vivo by deep sequencing of ribosome-protected mRNA fragments. Nat. Protoc. *7*, 1534–1550.

Jain, M., Nilsson, R., Sharma, S., Madhusudhan, N., Kitami, T., Souza, A.L., Kafri, R., Kirschner, M.W., Clish, C.B., and Mootha, V.K. (2012). Metabolite profiling identifies a key role for glycine in rapid cancer cell proliferation. Science *336*, 1040–1044.

Ji, Z., Song, R., Regev, A., and Struhl, K. (2015). Many lncRNAs, 5'UTRs, and pseudogenes are translated and some are likely to express functional proteins. eLife *4*, e08890.

Jiang, H.-Y., Wek, S.A., McGrath, B.C., Scheuner, D., Kaufman, R.J., Cavener, D.R., and Wek, R.C. (2003). Phosphorylation of the alpha subunit of eukaryotic initiation factor 2 is required for activation of NF-kappaB in response to diverse cellular stresses. Mol. Cell. Biol. *23*, 5651–5663.

(C) Immunoblot analysis of cytokine protein levels after 4 hr of glutamine deprivation and/or ISRIB treatment (250 nM).
(D) Microscopy images and quantification of cell migration through a basement toward a chamber with different test media. Error bars represent SD of three or more biological replicates. The p values are derived from the t test. n.s., not significant.
See also Figure S4.

Kim, M.-H., Kim, A., Yu, J.H., Lim, J.W., and Kim, H. (2014). Glutamine deprivation induces interleukin-8 expression in ataxia telangiectasia fibroblasts. Inflamm. Res. *63*, 347–356.

Larsson, O., Sonenberg, N., and Nadon, R. (2010). Identification of differential translation in genome wide studies. Proc. Natl. Acad. Sci. USA *107*, 21487–21492.

Maddocks, O.D.K., Berkers, C.R., Mason, S.M., Zheng, L., Blyth, K., Gottlieb, E., and Vousden, K.H. (2013). Serine starvation induces stress and p53-dependent metabolic remodelling in cancer cells. Nature *493*, 542–546.

Newsholme, E.A., Crabtree, B., and Ardawi, M.S. (1985). The role of high rates of glycolysis and glutamine utilization in rapidly dividing cells. Biosci. Rep. *5*, 393–400.

Reid, D.W., Chen, Q., Tay, A.S.-L., Shenolikar, S., and Nicchitta, C.V. (2014). The unfolded protein response triggers selective mRNA release from the endoplasmic reticulum. Cell *158*, 1362–1374.

Shanware, N.P., Bray, K., Eng, C.H., Wang, F., Follettie, M., Myers, J., Fantin, V.R., and Abraham, R.T. (2014). Glutamine deprivation stimulates mTOR-JNK-dependent chemokine secretion. Nat. Commun. *5*, 4900.

Sheen, J.-H., Zoncu, R., Kim, D., and Sabatini, D.M. (2011). Defective regulation of autophagy upon leucine deprivation reveals a targetable liability of human melanoma cells *in vitro* and *in vivo*. Cancer Cell *19*, 613–628.

Sidrauski, C., Acosta-Alvear, D., Khoutorsky, A., Vedantham, P., Hearn, B.R., Li, H., Gamache, K., Gallagher, C.M., Ang, K.K.H., Wilson, C., et al. (2013). Pharmacological brake-release of mRNA translation enhances cognitive memory. eLife *2*, e00498.

Singh, B., Tai, K., Madan, S., Raythatha, M.R., Cady, A.M., Braunlin, M., Irving, L.R., Bajaj, A., and Lucci, A. (2012). Selection of metastatic breast cancer cells based on adaptability of their metabolic state. PLoS ONE *7*, e36510.

Singleton, K.D., Beckey, V.E., and Wischmeyer, P.E. (2005). Glutamine prevents activation of NF-κB and stress kinase pathways, attenuates inflammatory cytokine release, and prevents acute respiratory distress syndrome (ARDS) following sepsis. Shock *24*, 583–589.

Tang, H., Hornstein, E., Stolovich, M., Levy, G., Livingstone, M., Templeton, D., Avruch, J., and Meyuhas, O. (2001). Amino acid-induced translation of TOP mRNAs is fully dependent on phosphatidylinositol 3-kinase-mediated signaling, is partially inhibited by rapamycin, and is independent of S6K1 and rpS6 phosphorylation. Mol. Cell. Biol. *21*, 8671–8683.

Thoreen, C.C., Kang, S.A., Chang, J.W., Liu, Q., Zhang, J., Gao, Y., Reichling, L.J., Sim, T., Sabatini, D.M., and Gray, N.S. (2009). An ATP-competitive mammalian target of rapamycin inhibitor reveals rapamycin-resistant functions of mTORC1. J. Biol. Chem. *284*, 8023–8032.

Thoreen, C.C., Chantranupong, L., Keys, H.R., Wang, T., Gray, N.S., and Sabatini, D.M. (2012). A unifying model for mTORC1-mediated regulation of mRNA translation. Nature *485*, 109–113.

Truitt, M.L., and Ruggero, D. (2016). New frontiers in translational control of the cancer genome. Nat. Rev. Cancer *16*, 288–304.

Vattem, K.M., and Wek, R.C. (2004). Reinitiation involving upstream ORFs regulates ATF4 mRNA translation in mammalian cells. Proc. Natl. Acad. Sci. USA *101*, 11269–11274.

Warburg, O., Wind, F., and Negelein, E. (1927). The metabolism of tumors in the body. J. Gen. Physiol. *8*, 519–530.

Wengrod, J., Wang, D., Weiss, S., Zhong, H., Osman, I., and Gardner, L.B. (2015). Phosphorylation of eIF2α triggered by mTORC1 inhibition and PP6C activation is required for autophagy and is aberrant in PP6C-mutated melanoma. Sci. Signal. *8*, ra27.

Wullschleger, S., Loewith, R., and Hall, M.N. (2006). TOR signaling in growth and metabolism. Cell *124*, 471–484.

Cell Reports, Volume *24*

Supplemental Information

Nutrient Deprivation Elicits a Transcriptional and Translational Inflammatory Response Coupled to Decreased Protein Synthesis

Paulo A. Gameiro and Kevin Struhl

Supplemental Experimental Procedures

Measurement of nascent protein synthesis. Protein synthesis was assessed using the 'clickable' methionine analog L-azidohomoalanine (AHA) that is incorporated into nascent proteins and detected by fluorescence microscopy according to the manufacturer's instructions (ThermoFisher scientific cat. No. C10289). Non-transformed and transformed cells were rinsed twice with warm PBS, and incubated with methionine-free medium (and lacking other nutrients as indicated) containing AHA for 30 minutes, 4 hours, or 6 hours at 37ºC in 5% CO_2. Cells were washed with PBS, fixed with 3.7 % formaldehyde, incubated with the Alexa Fluor 488 alkyne, and AHA-containing proteins were visualized using the 488nm laser channel. DAPI staining was performed to determine cell number. Quantification of protein synthesis was performed with MetaXpress Analysis Software (Molecular Devices) using custom cell scoring that consider the nuclei number, cell size and background correction for determination of average intensity of Alexa fluorescence per cell. We used ImageJ to set an equal minimum and maximum pixel intensity value in all RGB images for visualization of normalized fluorescence (Figure 1A). Three or more biological replicates were performed (6-12 imaging sites per replicate at 10X magnification) except for the 6 hours samples, no cysteine and no cystine condition at 30 minutes (two replicates).

Ribosome profiling and RNA sequencing. Non-transformed and transformed MCF10A-ER-Src cells were cultured with either complete or nutrient-deprived DMEM as indicated. For ribosome profiling, cells were washed with ice-cold PBS containing 100µg/ml cycloheximide, and flash-frozen with detergent lysis [20mM Tris-HCl (pH 7.4), 150mM NaCl, 5mM $MgCl_2$, 1mM DTT, 1% (vol/vol) triton X-100] containing 25 U/ml Turbo DNase I and 100µg/ml cycloheximide. Ribosome footprinting was performed by adding 8.75 µl of Rnase I (100 U/ml) to 350 µl of DNase I-treated lysates for 45 minutes at room temperature followed by addition of 12 µl of SUPERase·In inhibitor to stop the reaction. The Rna se I-digested lysates were added to 0.90 ml of 1M sucrose cushion, ribosomes were pelleted by centrifugation at 55,000 rpm at 4C overnight, resuspended in 700 µl of Qiazol reagent, and the RNA

isolated using the miRNeasy Kit (Qiagen, cat. no. 217004). Ribosome-protected fragments were PAGE purified on a 15% TBE-Urea gel (ThermoFisher scientific, cat. No. EC68852BOX), 3'end ligated to a pre-adenylated universal miRNA linker (5′-rAppCTGTAGGCACCATCAAT–NH2-3′, NEB, cat. no. S1315S), converted into cDNA using Superscript III reverse transcriptase (ThermoFisher scientific, cat. no. 18080-093), circularized, depleted for ribosomal RNA using biotinylated probes, and PCR amplified using Illumina TruSeq indexed primers as previously described (Ingolia et al., 2009, 2012). For RNA-seq, total RNA was extracted using the miRNeasy kit (Qiagen cat No. 217004), enriched for poly(A) RNA via three rounds of Oligo d(T)25 magnetic bead purification (NEB, cat. No. S1419S), fragmented with 10mM $ZnCl_2$ in 10mM Tris-HCl (pH 7.0) for 5 minutes at 80ºC, PAGE purified on a 15% TBE-Urea gel and processed equally as the ribosome protected fragments for Illumina TruSeq library preparation. The ribosome profiling and RNA-seq experiments were performed in duplicate with the exception of RNA-seq at 30 minutes (single experiments), ribosome profiling in cysteine/cystine-deprived EtOH cells (triplicate experiments), and the Torin1 dataset (single experiment). To process the data for both ribosomal profiling and RNA-seq, we first trimmed the adapter sequences from the raw sequencing reads, and mapped the reads to rRNA reference sequences. Non-ribosomal RNA reads were then aligned to the GENCODE (Harrow et al., 2012) defined transcripts and reference genome (hg19), and only the uniquely mapped reads were used for the subsequent calculations (Table S1). For determination of gene expression levels of protein coding genes, we removed refSeq defined coding regions overlapping with upstream open reading frames (uORFs) defined in (Ji et al., 2015), 15 amino acids downstream of start codons and 5 amino acids upstream stop codons. The gene expression levels were calculated as reads per kilobase of transcript per million mapped reads (RPKM) in the remaining coding regions.

Analyses of differential transcription and translation. For analysis of regulated mRNAs, we treated the 30 minutes and 4 hours datasets independently and considered only mRNAs expressed at RPKM > 10 in at least one condition in each dataset, which corresponds to 5,696 (30 minutes) and 6,478 (4 hours) translated ORFs (Table S1). We applied the exact Poisson test (poisson.test in R, two-sided) to

derive the statistical significance of ribosome occupancy (RO) counts between samples of interest, as follows: we compared the observed number of RO count events *x* (counts in gene *A* divided by total uniquely mapped counts in the nutrient-deprived condition) to the expected number of RO count events *T* (counts in gene *A* divided by total uniquely mapped counts in the complete DMEM condition) across all mRNAs. We defined transcriptional regulation as those mRNAs with an absolute log2 fold change in ribosome occupancy (RO) > 1.0 between the nutrient-deprived and complete DMEM condition and P value < 1e-03 (exact Poisson test). To define translational regulation, we used two analytical approaches. A) Translation efficiency (TE) was calculated as the log2 ratio of RPKM measured by ribosome profiling over RPKM measured by RNA-seq. We used the intersection of TE values with RO fold change to reject mRNAs with TE differences caused mostly by a decrease in mRNAs levels rather than an increase in RO upon the metabolic stress. An absolute difference in TE > 0.5, log2 RO fold change > 0.5 and P value < 1e-03 (exact Poisson test) between the nutrient-deprived and complete DMEM condition were used to define mRNAs with decreased translation, while a more stringent log2 RO fold change threshold (> 1.0) was applied along with the other criteria to define mRNAs with increased translation at 4 hours. B) We applied analysis of partial variance (APV) of normalized and rlog transformed RO and mRNAs levels and weighed the gene-specific variances using a random variance model to exclude possible correlations between mRNAs levels and TE values, as previously described (Larsson et al., 2010). Using the anota2seq package (Oertlin et al., 2018), mRNAs were defined as differentially translated if meeting the following criteria (-0.5 < minSlopeTranslation < 1.5, deltaP > 0.5, deltaPT > 0.15, FDR < 0.05). We applied a variance cutoff of 1e-06, and did not filter genes with zero counts to keep genes expressed in TAM but not in EtOH cells as input for APV.

Motif search, gene ontology and hierarchical clustering. We used RibORF (Ji et al., 2015) to define uORFs, and the MEME suite (Bailey et al., 2009) to performed an unbiased search for motifs in the 5'UTR of TE-regulated mRNAs. Enrichment of gene ontology (GO) terms in regulated mRNAs with corrected *P*-values (FDR, Benjamini and Hochberg) was determined using the ToppGene Suite (Chen

et al., 2009), and representative clusters of GO terms were found using REVIGO (Supek et al., 2011), with an 'allowed semantic similarity' of 0.4. Plotting in R was performed using the ggplot2 package (Wickham, 2009), and clustering analysis with the pheatmap package (Kolde, 2012). The ten metabolic conditions were clustered based on the normalized and rlog transformed RPKM values measured by ribosome occupancy of either all mRNAs (Figure 3E) or after aggregation of the mRNAs into 5 k-means (Figure 3F) using 'correlation' as a distance measure and the 'average linkage' method.

Immunoblotting. MCF10A-ER-Src cells were grown under different media, washed twice with PBS, lysed in RIPA buffer (150mM NaCl, 1.0% NP-40, 0.5% sodium deoxycholate, 0.1% SDS, 50mM Tris-HCl pH 8.0) supplemented with protease inhibitors, sonicated, and centrifuged. Supernatant proteins were separated by SDS-PAGE on a polyacrylamide gel (NuPAGE 4-12% Bis-Tris gel, ThermoFisher scientific), and transferred to a nitrocellulose membrane. The membrane was blocked with 5% milk (or 5% BSA for phosphorylated proteins) in TBS + 0.1% Tween-20 (TBS-T), incubated with primary antibody in blocking buffer overnight at 4C, washed 3X with TBS-T, incubated with a HRP-conjugated secondary mouse or rabbit antibody (Cell Signaling) in blocking buffer, and detected by enhanced chemiluminescence using either an X-ray film or a CCD camera. Primary antibodies: anti-phospho-eIF2α (Cell Signaling cat. No. 9721), anti-eIF2α (Cell Signaling), anti-phospho-p70 S6 kinase Thr389 (Cell Signaling, cat. No. 9205S), anti-phospho-4E-BP1 (Cell Signaling), anti-IL8 (ThermoFisher scientific cat. No. 14-7189-80), anti-IL6 (Novus Biologicals cat. No. NB600-1131SS), anti-CCL20 (antibodies-online GMBH cat. No. ABIN1043784, or ThermoFisher scientific cat. No. MA5-16253), anti-CXCL1 (Abcam cat. No. ab86436), anti-CXCL2 (Abcam cat. No. ab91511), anti-CXCL3 (Abcam cat. No. ab10064).

Wound-healing motility assay. A single scratch was created using a p20 micropipette tip in confluent non-transformed and transformed cells. Cells were washed with PBS and cultured with either complete, glutamine-free, or BCAA-free DMEM for 6 hours followed by complete DMEM for 24 hours. As negative control, ER-Src cells were cultured with serum-free DMEM for 30 hours. Triplicate

images were acquired by phase-contrast microscopy at 0 and 30 hours after wounding, and the percentage of gap closure was determined using TScratch (Gebäck et al., 2009). Three biological replicates were performed except for BCAA-deprived transformed cells (two experiments).

Transwell migration assay. MCF10A-ER-Src cells were trypsinized, resuspended in PBS, aliquoted (1E+05 cells) into complete or glutamine-free medium (200 µl) and seeded in the upper chamber of a Boyden insert placed inside 24 well plates. Conditioned-medium from cells grown in complete or glutamine-free DMEM was mixed with an equal volume of correspondent fresh medium, 750 µL added to the lower chamber, and cell migration via a membrane pore (8 µM) assessed after 18-20 hours of incubation. As control, fresh complete DMEM, glutamine-free DMEM or PBS were added to the lower chamber of other wells. Cells were fixed with 3.7% formaldehyde for 10 minutes, washed with PBS, permeabilized with 100% methanol for 20 minutes, washed with PBS, and stained with 0.1% crystal violet (CV) for 30 minutes at room temperature. After three PBS washes, non-migrated cells were scraped off the upper chamber with cotton swabs and dried. For quantification, we placed the Boyden chamber (containing the migrated cells) in 500 µl of 10% acetic acid to release the CV from cells, and measured absorbance at 590 nm. Relative cell migration was presented as the absorbance ratio of the conditioned medium relative to the respective fresh medium. Five and three biological replicates were performed in transformed and non-transformed cells, respectively.

FIGURE S1

A

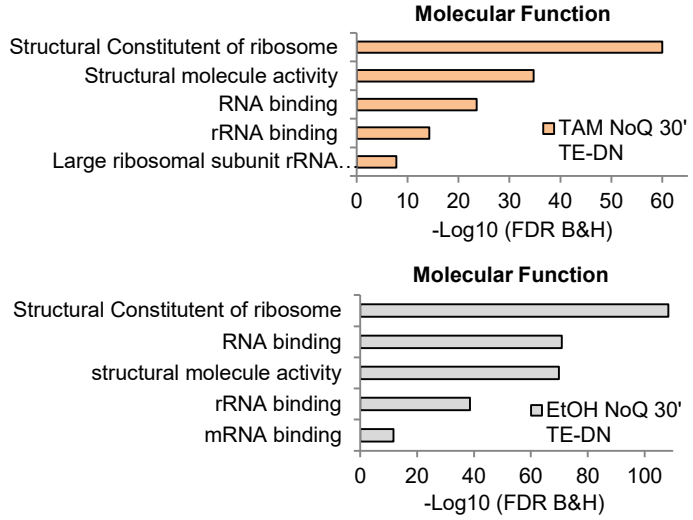

B

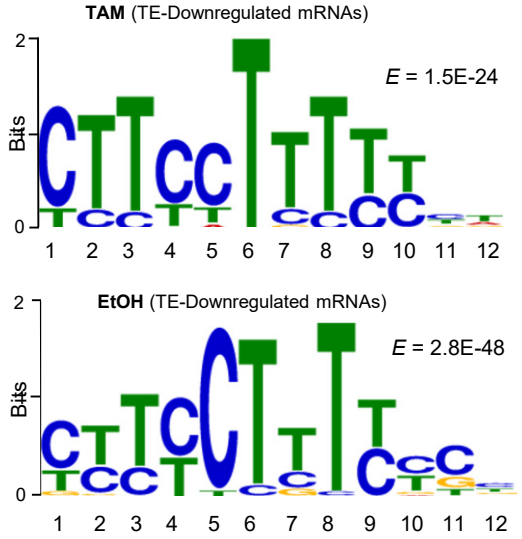

C

EtOH-treated – NoQ 4hrs	Analysis by Anota2seq – Ribosome occupancy UP ('Translated mRNA' Mode)			
term ID	description	log_{10} p-value	dispensability	N genes
GO:0036499	PERK-mediated unfolded protein response	-9.41	0.00	8
GO:0006915	apoptotic process	-7.19	0.05	36
GO:0072359	circulatory system development	-7.08	0.07	26
GO:0006357	regulation of transcription from RNA polymerase II	-7.67	0.18	37
GO:0006520	cellular amino acid metabolic process	-5.19	0.22	14
GO:0006984	ER-nucleus signaling pathway	-8.37	0.26	9
GO:0009628	response to abiotic stimulus	-5.58	0.26	25
GO:0042127	regulation of cell proliferation	-6.28	0.27	31
GO:0009719	response to endogenous stimulus	-5.49	0.35	30
GO:0034976	response to endoplasmic reticulum stress	-7.01	0.39	14

TAM-treated – NoQ 4hrs	Analysis by Anota2seq – Ribosome occupancy UP ('Translated mRNA' Mode)			
term ID	description	log_{10} p-value	dispensability	N genes
GO:0036499	PERK-mediated unfolded protein response	-11.98	0.00	10
GO:0072593	reactive oxygen species metabolic process	-6.06	0.02	15
GO:0006564	L-serine biosynthetic process	-6.20	0.05	4
GO:0042981	regulation of apoptotic process	-7.43	0.16	40
GO:0051240	positive regulation of multicellular organismal process	-6.97	0.23	40
GO:0009991	response to extracellular stimulus	-6.92	0.23	24
GO:0042127	regulation of cell proliferation	-6.27	0.23	39
GO:0006984	ER-nucleus signaling pathway	-9.96	0.26	11
GO:0071216	cellular response to biotic stimulus	-5.82	0.28	13
GO:0006955	immune response	-5.54	0.33	36
GO:0009607	response to biotic stimulus	-5.46	0.33	28
GO:0048585	negative regulation of response to stimulus	-6.75	0.33	38
GO:0009719	response to endogenous stimulus	-5.85	0.35	39
GO:0034976	response to endoplasmic reticulum stress	-7.88	0.39	18
GO:0044283	small molecule biosynthetic process	-5.75	0.39	21

D

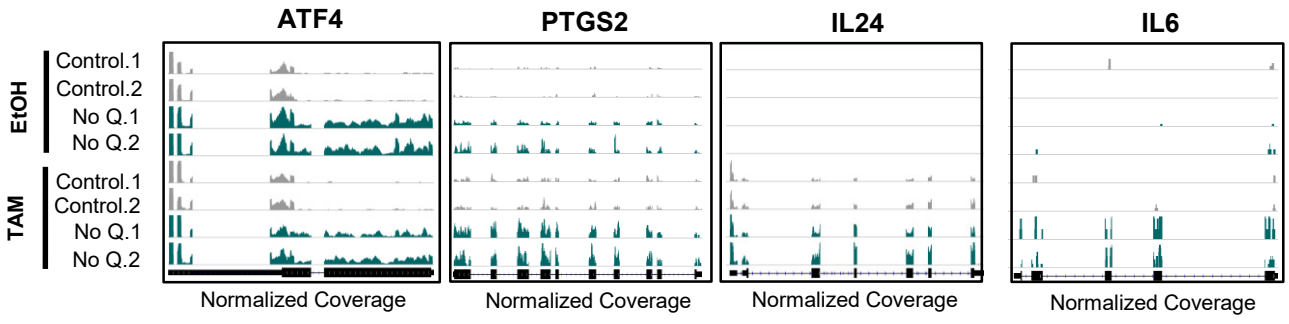

Figure S1; Related to figure 2: Regulation of mRNAs and their properties under glutamine-deprived transformed (TAM) and non-transformed (EtOH) MCF10A-ER-Src cells. (**A**) Gene ontology and (**B**) motif enrichment at 5' untranslated regions of mRNAs with decreased translation efficiency after 30 minutes. (**C**) Gene ontology of mRNAs with increased ribosome occupancy after 4 hours as determined by anota2seq ('translated mRNA mode'). (**D**) Ribosome occupancy of inflammatory mRNAs regulated after 4 hours.

FIGURE S2

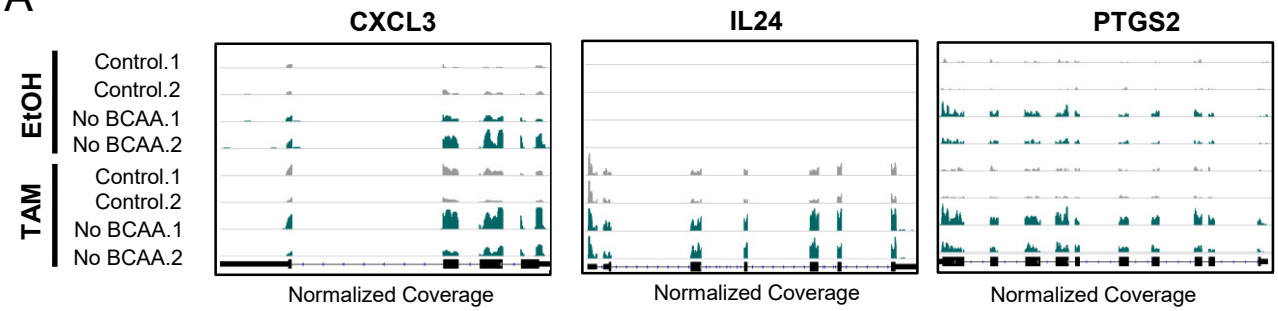

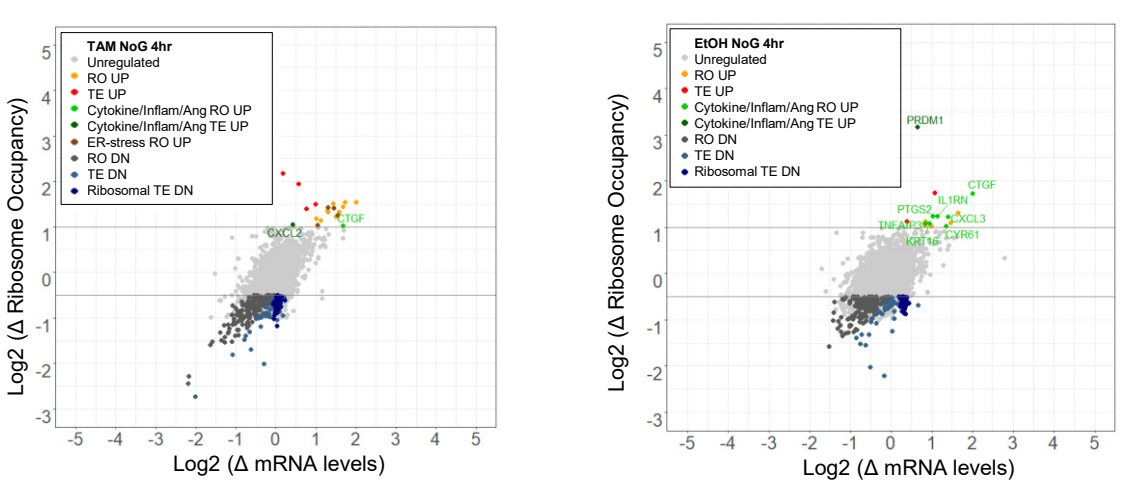

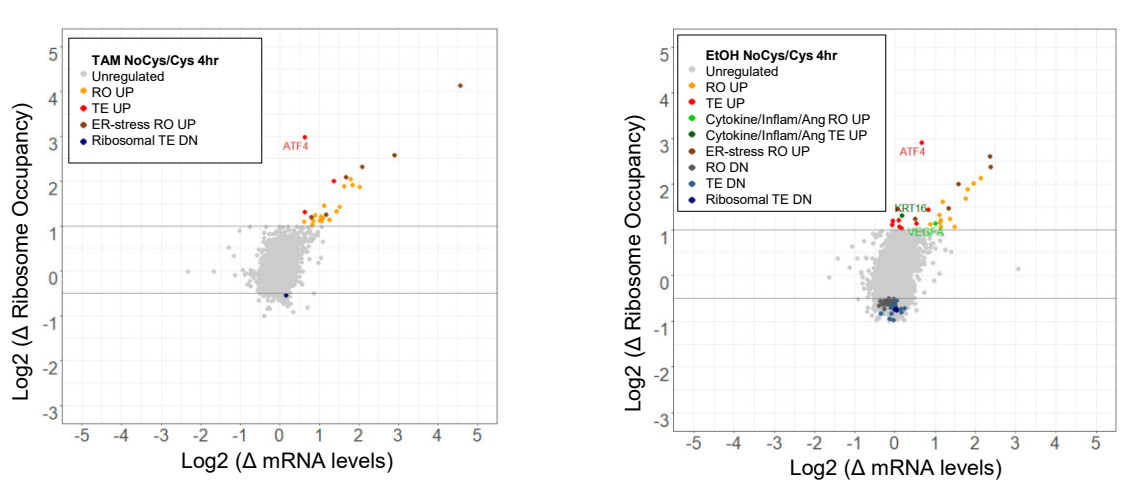

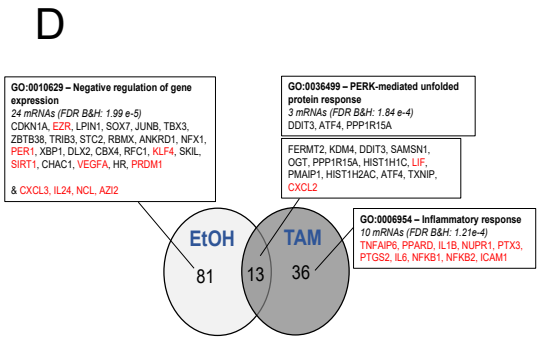

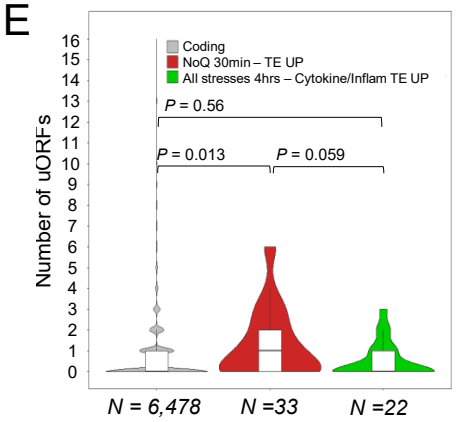

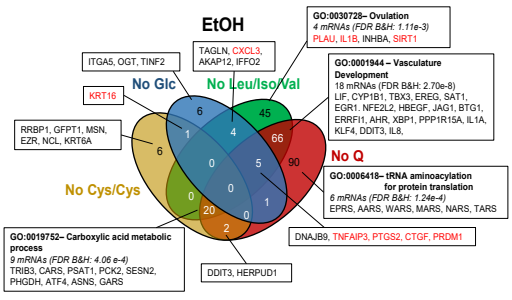

Figure S2; Related to Figure 3**:** Regulation of mRNAs in transformed and non-transformed MCF10A-ER-Src cells subjected to 4 hours of metabolic stress conditions. **(A)** Ribosome occupancy (RO) of inflammatory mRNAs after 4 hours of BCAA deprivation. (**B-C**) Changes in mRNA and RO levels upon 4 hours deprivation of (**B**) glucose and (**C**) cysteine/cystine relative to complete medium in transformed (left) and non-transformed (right) cells. (**D**) Venn diagram showing the mRNAs with increased translation efficiency (TE) in all metabolic stresses in transformed vs. non-transformed cells; cytokines highlighted in red. (**E**) Number of upstream open reading frames (uORFs) in all expressed coding mRNAs (grey), mRNAs with increased TE at 30 minutes of glutamine deprivation (red) and all inflammatory mRNAs with increased TE at 4 hours of nutrient deprivation (green). (**F**) Venn diagram showing the mRNAs with increased RO in each metabolic stress condition in non-transformed cells.

FIGURE S3

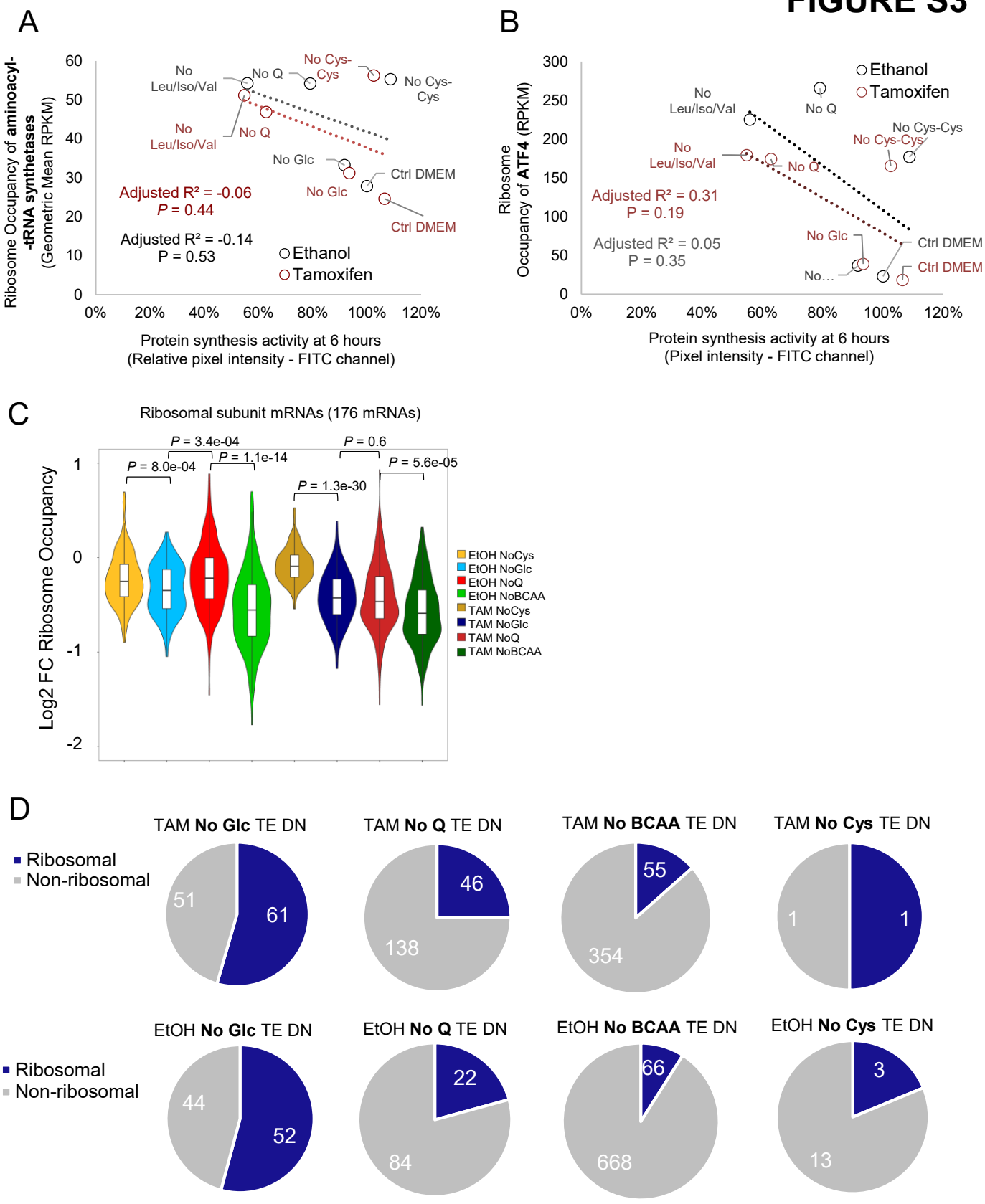

Figure S3; Related to Figure 3**:** Correlation between protein synthesis and the ribosome occupancy of (**A**) aminoacyl-tRNA-synthetases and (**B**) ATF4 in MCF10A-ER-Src cells. (**C**) Ribosome occupancy of all ribosomal subunit mRNAs in each metabolic condition; P values are derived from the Wilcoxon test. (**D**) Representation of ribosomal subunit mRNAs in the pool of mRNAs with decreased TE in each metabolic stress condition in MCF10A-ER-Src cells.

FIGURE S4

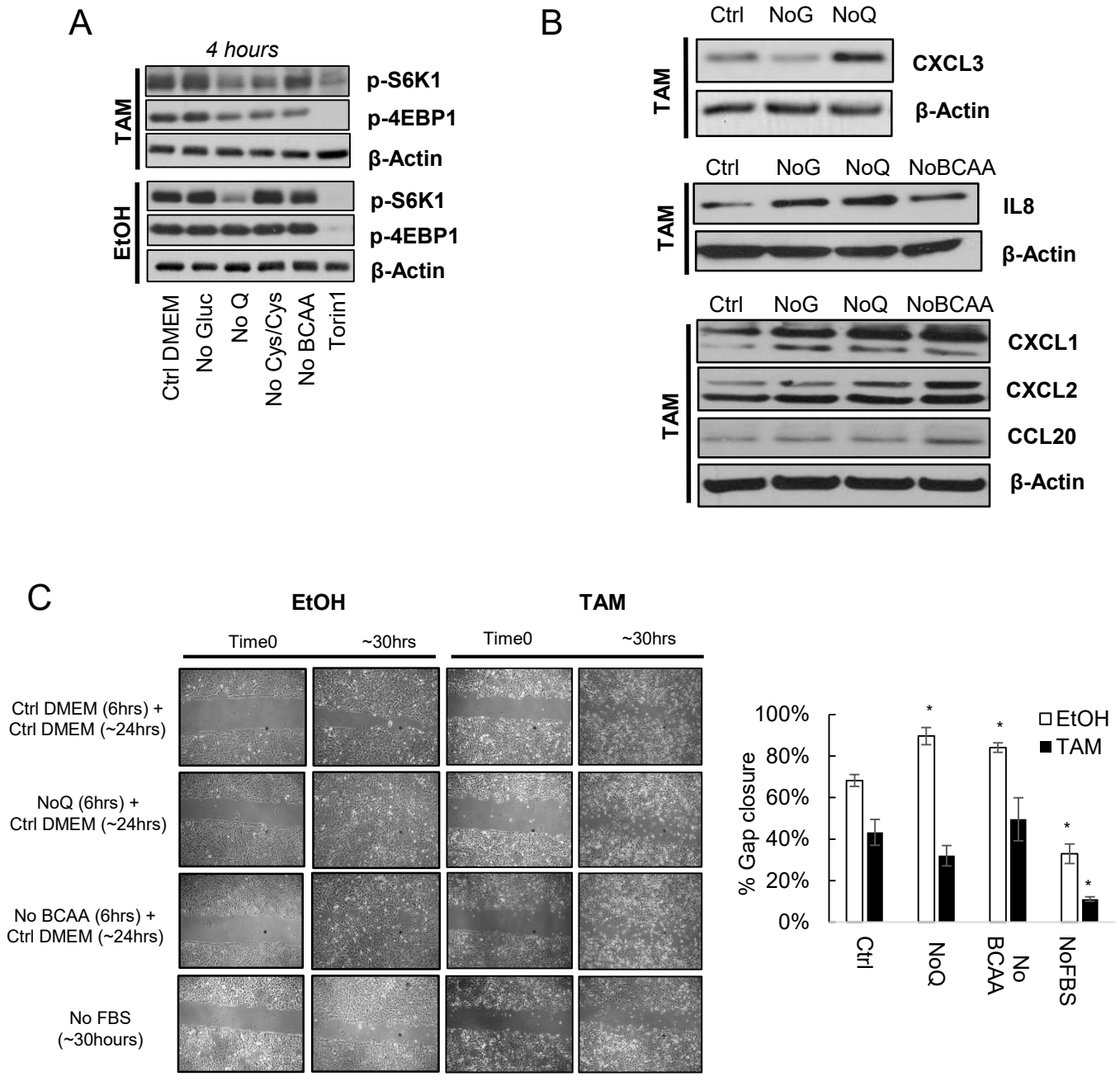

Figure S4; Related to Figure 4**:** Immunoblot analysis and cell motility assay of nutrient-deprived transformed (TAM) and non-transformed (EtOH) cells. (**A**) Immunoblot analysis of mTOR-phosphorylated proteins after 4 hours of nutrient deprivation or Torin1 treatment (500nM). (**B**) Immunoblot analysis of cytokine levels after 24 hours of nutrient deprivation (**C**) Phase-contrast images (left) and TScratch quantification (right) of nutrient-deprived cells in the wound healing assay. Error bars represent s.d. of three biological replicates (Control, NoQ, NoFBS) or two biological replicates (NoBCAA). * $P < 0.05$ comparing nutrient-deprived to complete medium as determined by t-test.

Supplemental References

Bailey, T.L., Boden, M., Buske, F.A., Frith, M., Grant, C.E., Clementi, L., Ren, J., Li, W.W., and Noble, W.S. (2009). MEME SUITE: tools for motif discovery and searching. Nucleic Acids Res. *37*, W202-8.

Chen, J., Bardes, E.E., Aronow, B.J., and Jegga, A.G. (2009). ToppGene Suite for gene list enrichment analysis and candidate gene prioritization. Nucleic Acids Res. *37*, W305-11.

Gebäck, T., Schulz, M.M.P., Koumoutsakos, P., and Detmar, M. (2009). TScratch: a novel and simple software tool for automated analysis of monolayer wound healing assays. Biotechniques *46*, 265–274.

Harrow, J., Frankish, A., Gonzalez, J.M., Tapanari, E., Diekhans, M., Kokocinski, F., Aken, B.L., Barrell, D., Zadissa, A., Searle, S., et al. (2012). GENCODE: the reference human genome annotation for The ENCODE Project. Genome Res. *22*, 1760–1774.

Ingolia, N.T., Ghaemmaghami, S., Newman, J.R.S., and Weissman, J.S. (2009). Genome-wide analysis in vivo of translation with nucleotide resolution using ribosome profiling. Science *324*, 218–223.

Ingolia, N.T., Brar, G. a, Rouskin, S., McGeachy, A.M., and Weissman, J.S. (2012). The ribosome profiling strategy for monitoring translation in vivo by deep sequencing of ribosome-protected mRNA fragments. Nat. Protoc. *7*, 1534–1550.

Ji, Z., Song, R., Regev, A., and Struhl, K. (2015). Many lncRNAs, 5'UTRs, and pseudogenes are translated and some are likely to express functional proteins. Elife *4*, e08890.

Kolde, R. (2012). Pheatmap: pretty heatmaps. R Packag. Version 61.

Larsson, O., Sonenberg, N., and Nadon, R. (2010). Identification of differential translation in genome wide studies. Proc. Natl. Acad. Sci. *107*, 21487–21492.

Oertlin, C., Lorent, J., Gandin, V., Murie, C., Masvidal, L., Cargnello, M., Furic, L., Topisirovic, I., and Larsson, O. (2018). Generally applicable transcriptome-wide analysis of translational efficiency using anota2seq. bioRxiv.

Supek, F., Bošnjak, M., Škunca, N., and Šmuc, T. (2011). REVIGO Summarizes and Visualizes Long Lists of Gene Ontology Terms. PLoS One *6*, e21800.

Wickham, H. (2009). ggplot2: Elegant Graphics for Data Analysis (Use R!) (Springer, New York).